Astron. Astrophys. 349, 907–911 (1999)

ASTRONOMY AND ASTROPHYSICS

2D radiative transfer with transiently heated particles for the circumstellar environment of Herbig Ae/Be stars

V. Manske and Th. Henning

Astrophysical Institute and University Observatory Jena, Schillergässchen 3, D-07745 Jena, Germany (manske, henning@astro.uni-jena.de)

Received 22 April 1999 / Accepted 21 May 1999

Abstract. We present results of self-consistent 2D radiative transfer calculations for Herbig Ae/Be stars. The emission from transiently heated particles and PAHs is included in these calculations. Special attention is paid to the influence of the model parameters on the strength of the PAH emission lines.

Our calculations show that appropriate 2D radiative transfer calculations are necessary in order to draw appropriate conclusions concerning the origin of the IR emission of Herbig Ae/Be stars and the mechanisms that may suppress the PAH emission lines. If one is concerned with the effect of accretion discs and transiently heated dust grains on the spectral energy distributions, 1D calculations can lead to inappropriate conclusions.

Furthermore, no combination of model parameters has been found that results in undetectably weak PAH emission lines. Hence, PAH emission should always be detectable in radiation from Herbig Ae/Be disk/envelope systems if PAHs are present in these systems.

Key words: radiative transfer – methods: numerical – stars: emission-line, Be – ISM: dust, extinction – ISM: molecules – infrared: stars

1. Introduction

Herbig Ae/Be stars form a class of intermediate-mass pre-main sequence stars, which has attracted much attention because it forms the bridge between the low-mass T Tauri stars and high-mass young stellar objects (for reviews see Pérez & Grady 1997, Waters & Waelkens 1998, Natta et al. 1999). The dust continuum radiation of these objects has been related to disks and/or envelopes (see, e.g., Henning et al. 1994, 1998; Natta et al. 1999). Hillenbrand et al. (1992) introduced a classification scheme (the "groups" 1, 2, and 3) based on the slope of the continuum spectral energy distributions (SEDs) in the infrared.

Hartman et al. (1993) and Natta et al. (1993) found that the SEDs of some Herbig Ae/Be stars (hereafter HAEBE stars) show evidence for the presence of very small dust grains (VSGs) that undergo temperature fluctuations. Based on 1D radiative transfer calculations, Natta et al. (1993) concluded that SEDs of HAEBE stars with a dusty envelope, containing VSGs, are similar to the SEDs of HAEBE stars with accretion discs.

The SEDs of at least 20% of all HAEBE stars show PAH emission lines (Brooke et al. 1993). The non-detection of PAH emission in most of the pre-ISO observations of HAEBE stars is after Natta & Krügel (1995) either a result of using too small telescope beams for the observations or due to the suppression of the PAH emission by the radiation of the central star or an accretion disc. However, almost all HAEBE stars investigated by ISO show PAH emission lines if the objects are associated with reflection nebulosities (Natta et al. 1999).

The aim of this paper is to check, whether the results obtained with 1D radiative transfer calculations are consistent with the results of 2D calculations or not. Special attention is paid to the influence of accretion discs and VSGs on the continuum SED of HAEBE stars. Furthermore, the detectability of PAH line emission in HAEBE stars is investigated. Modeling results for individual object, using ISO and ground-based data, will be presented in a subsequent paper.

In Sect. 2, we describe the radiative transfer code, the physical model of the HAEBE stars, and the model parameters. In Sect. 3 we present and discuss our results. The paper is finished with our conclusions (Sect. 4).

2. Modeling

To model the emission of HAEBE stars, we used the 2D radiative transfer code of Manske & Henning (1998). This code calculates the continuum radiative transfer for spherically symmetric envelopes (1D) and flared dust discs (2D) and includes a treatment of VSGs and PAHs.

The physical model for HAEBE stars used in this work consists of a central star which is surrounded by an inner accretion disc and an outer envelope with polar cavities responsible for the PAH emission. The outer radius of the dust envelope is set to 10^4 AU (see Table 1) and its inner radius is 100 AU. The accretion disc is assumed to be an optically thick and geometrically thin "standard" stationary Keplerian disc ("α-disc", Frank et al. 1992). The radius of the disc is chosen to be 100 AU, in rough agreement with recent interferometric observations (Mannings & Sargent 1997, Mannings et al. 1997). The combination of the central star and the accretion disc powers the IR emission of the envelope. A "back-heating" from the envelope onto the accretion disc is not taken into account. For a detailed descrip-

Table 1. "Grid points" of the investigated parameter space. The optical depth is measured in radial direction in the envelope midplane.

stellar temperature	$T_\star/10^3 = 8, 10, 15, 20$ K
stellar luminosity	$L_\star/L_\odot$ = 1, 100, 1000, 10^4
density distribution	$\rho(r) \propto r^{-\beta}$, $\beta = 0.5, 1.5$
optical depth	$\tau_{550\mathrm{nm}} = 0.3, 1, 3, 10$
accretion disc luminosity	$L_{\mathrm{acc}} = \gamma \cdot 10^3 L_\odot$, $\gamma = 0, 1, 3, 6$
envelope opening angle	$\Psi = 40^\circ, 90^\circ, 150^\circ$
fraction of small particles	$\alpha = \frac{M_{\mathrm{small}}}{M_{\mathrm{big}}} = 0, 0.1, 0.3, 1$

Table 2. Parameters of the standard model

stellar temperature	$T_\star = 20000$K
stellar luminosity	$L_\star = 10^4 L_\odot$
density distribution	$\rho(r) \propto r^{-0.5}$
envelope opening angle	$\Psi = 150^\circ$
envelope radius	$R_{\mathrm{max}} = 10^4$AU
optical depth	$\tau_{550\mathrm{nm}} = 1$
luminosity of accretion disc	$L_{\mathrm{acc}} = 0$
fraction of small particles	$\alpha = \frac{M_{\mathrm{small}}}{M_{\mathrm{big}}} = 0.3$

tion of the treatment of the star/disc/envelope system, we refer to Manske et al. (1998). For all calculations, we assumed the star/disc/envelope system to be at a distance of 140 pc.

To investigate the influence of the model parameters on the SED and the PAH emission, we varied the stellar temperature and luminosity, the angle of the line of sight (in relation to the envelope midplane), the envelope opening angle, the radial density distribution, the optical depth of the envelope, the accretion disc luminosity, and the dust opacity (Table 1). In total we calculated more than 100 models (see Table 1 for details) with different combinations of model parameters to obtain the SEDs for face-on ($\Phi = 90^\circ$; line of sight towards one of the cavities) and edge-on ($\Phi = 0^\circ$) lines of sight. For simplicity, we discuss only models where the results are significantly different from the results of the "standard" model (Table 2). The parameters of the standard model are more or less arbitrarily chosen from the parameters in Table 1. However, this choice has no influence on the discussed results.

The dust used in this work is composed of silicate, graphite, and amorphous carbon grains with the optical data from Dorschner et al. (1995), Draine (1985), and Preibisch et al. (1993), respectively, as well as of PAHs (Schutte et al. 1993). According to chemical composition and heating mechanism, we have five distinct dust components:

1. Big silicate grains with radii between 0.01 and 0.5 μm.
2. Big amorphous carbon grains (0.01 to 0.5 μm).
3. Very small silicate grains (0.001 μm (10 Å) to 0.01 μm (100 Å))
4. Very small graphite grains (0.001 μm (10 Å) to 0.01 μm (100 Å))
5. Compact PAH molecules, composed of 30 to 500 carbon atoms, with a degree of dehydrogenation of 90%, with the absorption cross sections from Schutte et al. (1993).

The power-law index q of the grain size distribution ($n(a) \propto a^{-q}$, $a_{\mathrm{min}} \leq a \leq a_{\mathrm{max}}$) is set to 4, for all five dust components. The silicate to carbon mass-ratio is 1:1. In the standard model the ratio of masses of VSGs M_{small} to big grains M_{big} is $M_{\mathrm{small}} : M_{\mathrm{big}} = 1 : 3$. The amount of PAHs is assumed to be 3% of the mass of the total carbon content of the dust torus, being fairly in agreement with estimates by Pendleton et al. (1994).

3. Results and discussion

General remark: Almost all presented SEDs show a strong 10 μm silicate emission feature, produced by the small silicate grains, that is not always clearly observed, but present in many cases (Wooden 1994, Malfait et al. 1999). However, the silicate content of the envelope has only little influence on the continuum SED, and is therefore not relevant for the following discussions. In addition, ISO observations show the presence of a variety of crystalline silicates which have to be considered for a detailed modeling of individual objects (Malfait et al. 1998, 1999).

In Figs. 1 A1/2 we present the SEDs obtained for the standard model for different viewing angles (face-on: $\Phi = 90^\circ$, edge-on: $\Phi = 0^\circ$). In Fig. 1 A2 we give a "zoom-view" on the PAH emission lines. The presented continuum SEDs differ a lot at visible wavelengths, but they are almost identical at infrared wavelengths. This is due to the fact that the dust envelope is optically thin for IR photons ($\tau_{3.3\,\mu\mathrm{m}} = 0.06$). Hence, the strength of the PAH lines is nearly independent of the viewing angle. Therefore, we restrict our presentation on the results obtained for the face-on line of sight.

The results for different stellar temperatures are shown in Fig. 1 B. Decreasing the temperature from 20.000 K to 8.000 K decreases the energy of the photons emitted by the star. This mainly reduces the strength of the most-energetic PAH line, the 3.3 μm line, by almost 50%. The other PAH lines show only a flux reduction of about 10% (see Table 3). As the luminosity of the star is kept constant for these calculations, the underlying continuum changes only little.

The effects are a bit different if the stellar luminosity is decreased from 10^4 to 10 solar luminosities (Fig. 1 C), while keeping the stellar temperature at $2 \cdot 10^4$K. Now, the strength of the lowest energetic PAH lines are also strongly reduced. The strength of the 11.3 μm line decreases by about 50%, if the fluxes are corrected for the lower luminosity (Table 3). The mid-energetic lines at 6.2 and at 7.6 μm show a surprisingly small increase, as a result of the lower dust continuum emission. The reduction of the continuum emission follows from lower dust temperatures because of the decrease in stellar luminosity.

In Fig. 1 D1/2 we plotted the SEDs obtained for different optical depths. Although the continuum SEDs differ quite strongly if the optical depth is varied, these variations have only little influence on the strength of the PAH emission lines (see Table 3), if the different dust masses are taken into account. Even if the dust mass, and therefore the PAH content, is varied by a factor of 3 to 10, the PAH line flux changes only by at least 60%. This indicates, that a higher optical depth (lower UV-penetration of

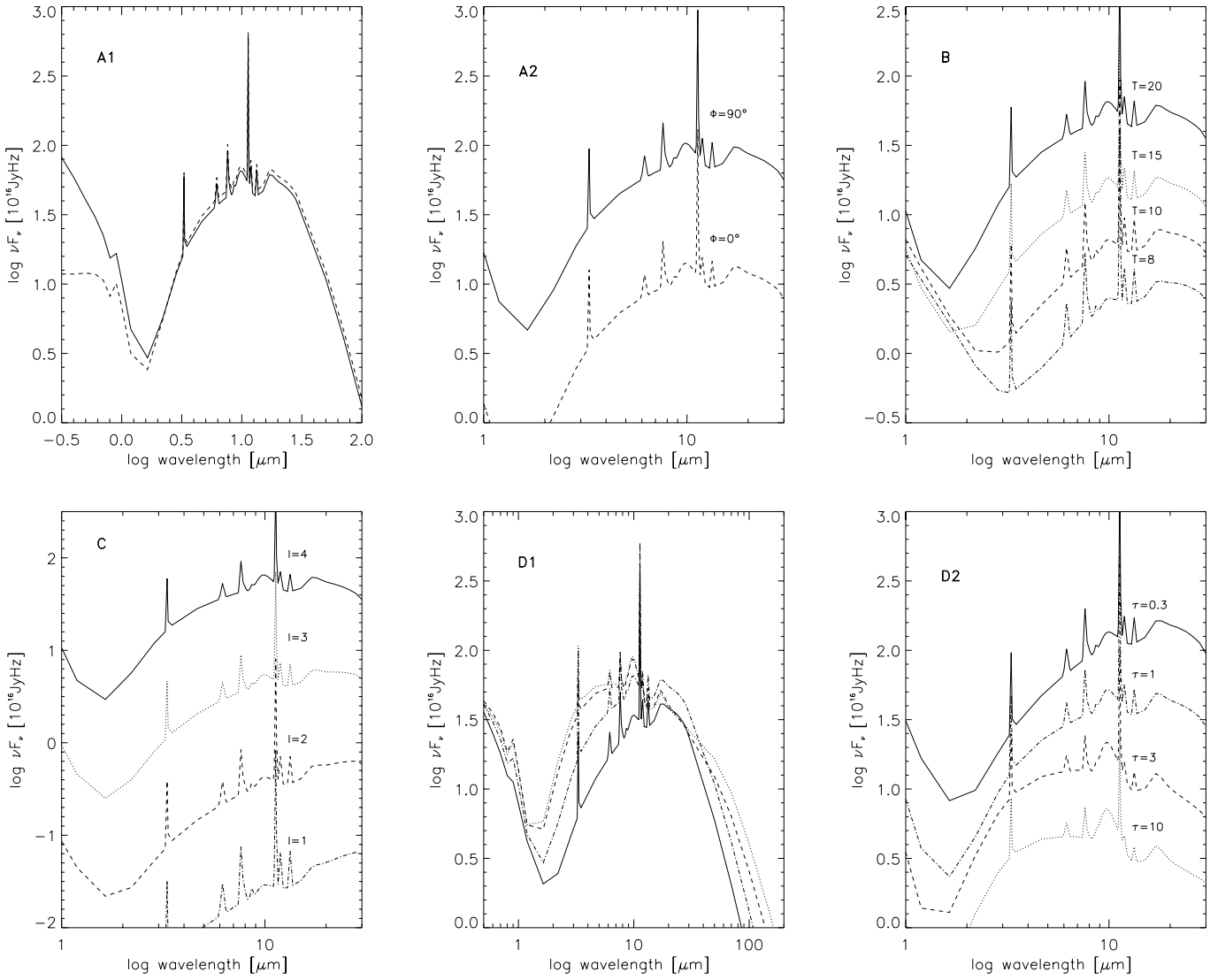

Fig. 1. A1/A2: SEDs for the standard model for different viewing angles. B: SEDs for models with different stellar temperatures T in 10^3 K. C: SEDs for models using various stellar luminosities $L = 10^l L_\odot$. D1/D2: SEDs for envelopes with different optical depth ($\tau = \tau_{550\mathrm{nm}}$), measured in radial direction in the envelope midplane. Please note that for the clarity of the presentation the SEDs shown in frame A2, B and D2 are arbitrarily shifted along the y-axis.

the envelope) is mainly balanced by a higher PAH content. In opposite, the lower PAH content for lower optical depth models is balanced by a higher UV-penetration.

The resulting model SEDs for different accretion disc luminosities are shown in Fig. 2 A1/A2. These results clearly contradict the suggestion of Natta & Krügel (1995) that the PAH emission lines in HAEBE star SEDs could be suppressed by the continuum emission of an inner accretion disc. Even for models with highly luminous accretion discs the PAH line strength changes only by about 2% (Table 3), although the continuum emission of HAEBE depends very much on accretion disc luminosities. This result clearly indicates that self-consistent 2D radiative transfer calculations are needed to understand the nature and origin of the IR emission of HAEBE stars. As we have demonstrated, results obtained with 1D codes may lead to partially misleading conclusions.

In Figs. 2 B1/2, we compare the SEDs of 1D models with/without VSGs and PAHs with the results of 2D calculations for HAEBE stars with accretion discs and VSGs and PAHs. It follows that taking into account the emission of VSGs in 1D calculations leads to continuum SEDs that are similar to 2D "face-on" SEDs obtained for models with accretion discs. Such a similarity was proposed by Natta & Krügel (1995), based on 1D radiative transfer calculation. This suggestion is now confirmed by 2D radiative transfer calculations that include a treatment of VSGs and PAHs. It is remarkable that also the strengths of the PAH emission lines are almost the same for the 1D and the 2D configurations. However, this changes if envelopes with higher optical depth are used. Then, 2D models produce signif-

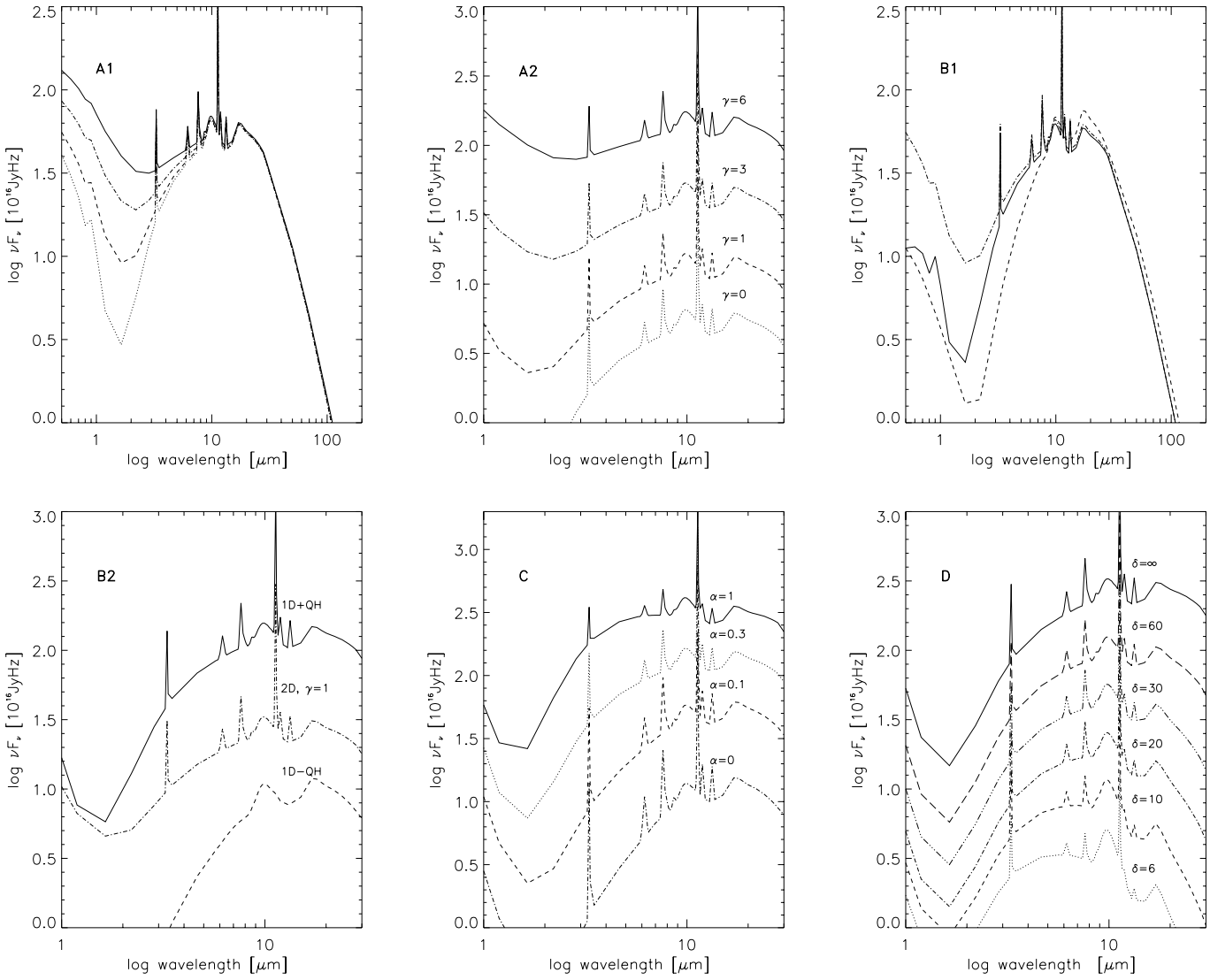

Fig. 2. A1/A2: Effect of accretion disc luminosity on the model SED ($L_{\rm acc} = \gamma \cdot 10^3 L_\odot$). B1/B2: Comparison of the effect of VSGs and PAHs on the SEDs for 1D and 2D models. 1D+QH: 1D model with VSGs and PAHs. 1D-QH: 1D model without VSGs and PAHs. 2D $\gamma = 1$: 2D model with VSGs and PAHs and an accretion disc. C: Effect of mass ratio of VSGs on the SED and the PAH emission lines. D: Effect of different telescope beam sizes (δ, measured in arcsec) on the strength of the PAH emission lines. Please note that for the clarity of the presentation the SEDs shown in frame A2, B2, C and D are arbitrarily shifted along the y-axis.

Table 3. Variation of PAH line strength for different model parameters. The row "standard model" contains the model center PAH line fluxes in 10^{16}JyHz, obtained after subtraction of the underlying continuum for the most prominent PAH lines. "Min" and "Max" denotes the deviation of the lowest and highest obtained PAH line flux values from the standard model PAH line flux values. The comparison of the data for different stellar luminosities was done by dividing the PAH line fluxes by the stellar luminosity.

PAH line	3.3 μm		6.2 μm		7.6 μm		11.3 μm	
standard model	43.1		15.2		43.5		542.7	
	Min	Max	Min	Max	Min	Max	Min	Max
stellar luminosity $L_\star$	-37%	+0%	+1%	-0%	-1%	+10%	+50%	-0%
stellar temperature $T_\star$	-47%	+0%	+1%	-16%	+2%	-9%	+4.5%	-8%
opt. depth $\tau_{550\rm nm}$	-60%	+33%	-4%	+0%	-42%	+0%	-35%	+0%
accretion disc γ	-2%	+2%	-2%	+2%	-2%	+2%	-2%	+2%
ratio of small grains α	-38%	+18%	-39%	+40%	-41%	+44%	-43%	+51%
telescope beam size δ	-48%	+0%	-70%	+0%	-80%	+0%	-86%	+0%

icantly higher PAH line fluxes than 1D models with the same model parameter values.

The effect of VSGs on the model SED is illustrated in Fig. 2 C. Apart from significantly increasing the near- to mid-IR flux ($1 < \lambda < 10\mu$m), an increase of the mass ratio of VSGs decreases the strength of the PAH lines. The VSGs simply "overshine" the emission of the PAHs because the PAH emission is more spatially concentrated than the emission of the small particles. UV photons are needed to stimulate the line emission of the PAHs. Interestingly, small particles in dust envelopes around HAEBE stars lead to exactly the PAH emission "suppressing effect" that Natta & Krügel (1995) have proposed for HAEBE stars with accretion discs. However, even for very high, probably unrealistically high, values of α the PAH lines are clearly visible.

In Fig. 2 D, the effect of different telescope beam sizes is shown. As expected, the PAH line fluxes decrease significantly if the beam size is reduced. However, the PAH line flux is not proportional to the beam size. For instance, the maximum line strength decrease at 3.3 μm is only 48%, while reducing the beam size by a factor of more than 10. Although the strength of the PAH line emission decreases with decreasing beam size, the PAH emission is clearly detectable, even for very small telescope beams (high-resolution observations).

4. Conclusion

Our investigation of the parameter space for dust envelopes around HAEBE stars has demonstrated that no combination of model parameters leads to a complete suppression of the PAH emission. Even the presence of high-luminosity accretion discs, a high amount of VSGs, dust envelopes with a high optical depth, or the use of small telescope beam sizes cannot prevent the PAH emission from appearing in the model SEDs. Therefore, we conclude that a possible non-detection of PAH emission in HAEBE star SEDs is either a result of regional differences in PAH opacities (mainly the UV absorption cross section), a lack of PAHs in the envelope, or a too-low spectral resolution of the observations. The latter assumption is supported by the detection of PAH emission in all HAEBE star SEDs investigated by ISO (Waelkens et al. 1996). However, we should note that the PAH emission seems to be more correlated with the presence of reflection nebulosities (Natta et al. 1999).

Furthermore, our calculations clearly show that 2D radiative transfer calculations that consider the emission of transiently heated small dust particles and PAHs are necessary to understand the origin of the IR emission of Herbig Ae/Be stars. The use of 1D codes may lead to inappropriate conclusions.

Acknowledgements. We like to thank D. Jones and X. Etra for their financial support of one of the authors.

References

Brooke T.Y., Tokunaga A.T., Strom S.E., 1993, AJ 106, 656
Dorschner J., Begemann B., Henning Th., Jäger C., Mutschke H., 1995, A&A 300, 503
Draine B.T., 1985, ApJS 57, 587
Frank J., King A., Raine D., 1992, Accretion power in astrophysics. Cambridge University Press, Cambridge, p. 77ff
Hartman L., Kenyon S., Calvet N., 1993, ApJ 407, 219
Henning Th., Launhardt R., Steinacker J., Thamm E., 1994, A&A 291, 546
Henning Th., Burkert A., Launhardt R., Leinert Ch., Stecklum B., 1998, A&A 336, 565
Hillenbrand L.A., Strom S.E., Vrba F.J., Keene J., 1992, ApJ 397, 613
Malfait K., Waelkens C., Waters L.B.F.M., et al., 1998, A&A 332, L25
Malfait K., Waelkens C., Bouwman J., Koter A., Waters L.B.F.M., 1999, A&A 345, 181
Mannings V., Sargent A., 1997, ApJ 490, 792
Mannings V., Koerner D.W., Sargent A., 1997, Nat 388, 555
Manske V., Henning Th., 1998, A&A 337, 85
Manske V., Henning Th., Men'shchikov A.B., 1998, A&A 331, 52
Natta A., Krügel E., 1995, A&A 302, 849
Natta A., Prusti T., Krügel E., 1993, A&A 275, 533
Natta A., Grinin V.P., Mannings V., 1999, In: Mannings V., Boss A., Russell S. (eds.) Protostars and Planets IV, University of Arizona Press, in press
Pérez M.R., Grady C.A., 1997, Space Sci. Rev. 82, 407
Pendleton Y.J., Sandford S.A., Allamandola L.J., et al., 1994, ApJ 437, 683
Preibisch Th., Ossenkopf V., Yorke H., et al., 1993, A&A 279, 577
Schutte W.A., Tielens A.G.G.M., Allamandola L.J., 1993, ApJ 415, 397
Waters L.B.F.M., Waelkens C., 1998, ARA&A 36, 233
Waelkens C., Waters L.B.F.M., de Graauw M.S., et al., 1996, A&A 315, L245
Wooden D.H., 1994, In: Thé P.S., Pérez M.R., Heuvel E.P.J. (eds.) The Nature and Evolutionary Status of Herbig Ae/Be stars. ASP Conf. Ser. 62, 138